bation mixtures containing nonradioactive inactivators. The exact amounts of CO_2 released during inactivation varied among enzyme preparations,[49] but the values reported in the text represent the average of two experiments for each inactivator. The original amount of active MAO was determined by titration with [^{3}H]pargyline.[46] Calculated stoichiometries were corrected for any remaining MAO activity and are expressed as mole of radiolabel bound per mole of inactivated MAO.

Identification of the Amount of Non-Amine Metabolites. Following incubation of MAO (44 μL of a 0.3 mg/mL enzyme solution) for 29 h with either the ^{14}C- or ^{3}H-labeled **15** (R = 3-ClPh) (965 μL of a 105 μM solution), the incubation mixture was placed directly onto a column (0.5 × 8.5 cm) of Dowex 50X-8 (200–400 mesh, H^+ form) equilibrated with deionized water. The column was eluted with deionized water (40 mL), and the eluent was collected in eight 10-mL scintillation vials. The eluent was analyzed for radioactivity by liquid scintillation counting. The amount of non-amine metabolites was determined by comparison to control values from a column run on a similar solution of inactivator incubated without MAO. The original amount of active MAO was determined by titration with [^{3}H]pargyline.[46] Calculated stoichiometries were corrected for any remaining MAO activity and are expressed as mole of radiolabel bound per mole of inactivated MAO.

Flavin Spectra of MAO Inactivated by 15 (R = H). MAO (45 μL) was incubated for 15 h in a 50 mM solution of **15** (R = H) (405 μL) (final concentration of MAO 11 μM). An assay showed that the enzyme was over 90% inactivated after that time period. The incubation mixture and a control that was incubated with buffer excluding inactivator were placed in dialysis bags and dialyzed (3 × 200 mL) against 100 mM NaP_i pH 7.2 buffer at room temperature. The dialyzed MAO solutions were placed in cuvettes and the spectra (350–550 nm) were recorded. After denaturation by addition of 13 μL of 30% sodium dodecyl sulfate, the spectra of the inactivated and control enzyme were again recorded.

(49) Although the exact amounts of radioactivity varied with different enzyme preparations, in all parallel inactivation experiments, equivalent amounts of ^{3}H and ^{14}C were incorporated into the enzyme by the correspondingly labeled inactivator analogues.

Acknowledgment. We are grateful to the National Institutes of Health (Grant GM32634) for financial support of this research.

Kinetic Energy Release Distributions as a Probe of Ligation Effects on Potential Energy Surfaces in Organometallic Reactions. Reversible Dehydrogenation of Cycloalkenes by Fe^+

David V. Dearden,[‡] J. L. Beauchamp,*[,‡] Petra A. M. van Koppen,*[,§] and Michael T. Bowers*[,§]

Contribution from the Arthur Amos Noyes Laboratory of Chemical Physics, California Institute of Technology,[†] Pasadena, California 91125, and Department of Chemistry, University of California, Santa Barbara, California 93106. *Received April 9, 1990*

Abstract: The kinetic energy release distributions associated with dehydrogenation and double-dehydrogenation processes for Fe^+ reacting with cyclopentene, cyclohexene, cyclopentane, and cyclohexane have been obtained. Previously, dehydrogenation of alkanes and alkenes by Co^+ and Ni^+ in the gas phase has been characterized by release of more energy into product translation than can be accounted for by statistical theory. This observation is not general, however, since here we show dehydrogenations of cyclopentene and cyclohexene by Fe^+ are well described by statistical phase-space theory with the best fit of theory to experiment yielding $D_0°(Fe^+–C_5H_6) = 50 \pm 5$ kcal/mol and $D_0°(Fe^+–C_6H_8) = 66 \pm 5$ kcal/mol. For statistical theory to be applicable, it is required that there be no barrier for the reverse association reaction. The absence of a barrier in these systems is consistent with studies that indicate H/D exchange for $Fe(C_5H_6)^+$ is reversible and occurs in the presence of excess D_2 at about 5% of the Langevin collision rate. The product kinetic energy release distributions measured for the final hydrogen loss in the double dehydrogenations of cyclopentane and cyclohexane by Fe^+ are remarkably similar to those obtained for single dehydrogenations of cyclopentene and cyclohexene. This similarity is explained by participation of electronically excited Fe^+ in the first step of the double-dehydrogenation processes, which supplies the additional energy required to observe the second H_2 loss as a metastable process.

Introduction

The dehydrogenation of hydrocarbons by transition-metal ions has been extensively investigated. From studies of isotopically labeled butanes, it has been established that at least two distinct dehydrogenation mechanisms are operative. The reactions of Co^+ and Ni^+ with 2-methylpropane-*2-d_1* result in exclusive loss of HD, indicating that 1,2-dehydrogenation is the dominant route.[1] Ion-beam studies[1,2] of the dehydrogention of butane-*1,1,1,4,4,4-d_6* by Ni^+, as well as ligand exchange[2] and low-energy collision-induced dissociation experiments,[3] indicate that 1,4-dehydrogenation is the main process in that system. The reaction of Co^+ with butane-*1,1,1,4,4,4-d_6* gives a mixture of dehydrogenation products, with losses of H_2, HD, and D_2 occurring with ratios 20:35:45.[1] When the kinetic energy release distributions (KERDs) from selectively deuterated butanes were compared it was concluded[4] that 1,4-elimination was occurring, and H/D scrambling before hydrogen elimination yielded the observed isotopic ratios. The KERDs from Co^+ reacting with various isomeric butanes were distinct for 1,2- and 1,4-dehydrogenations and were all much broader than predicted by statistical theory, a result that appeared at that time to be general for dehydrogenation reactions.

[†] Contribution No. 8109 from the California Institute of Technology.
[‡] California Institute of Technology.
[§] University of California.

(1) Houriet, R.; Halle, L. F.; Beauchamp, J. L. *Organometallics* **1983**, *2*, 1818–1829.
(2) Halle, L. R.; Houriet, R.; Kappes, M. M.; Staley, R. H.; Beauchamp, J. L. *J. Am. Chem. Soc.* **1982**, *104*, 6293–6297.
(3) (a) Jacobson, D. B.; Freiser, B. S. *J. Am. Chem. Soc.* **1983**, *105*, 5197–5206. (b) Jacobson, D. B.; Freiser, B. S. *J. Am. Chem. Soc.* **1983**, *105*, 736.
(4) Hanratty, M. A.; Beauchamp, J. L.; Illies, A. J.; van Koppen, P.; Bowers, M. T. *J. Am. Chem. Soc.* **1988**, *110*, 1–14.

0002-7863/90/1512-9372$02.50/0

Scheme I. Mechanism Proposed for H/D Exchange in $M(C_5H_6)^+$ Species in the Presence of Excess D_2, Where M = Fe and Co

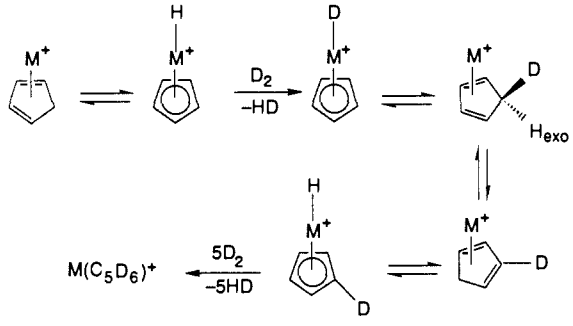

KERDs substantially broader than predicted by statistical theory have been interpreted as evidence of a barrier in the potential energy surface exit channel leading to product formation.[4,5] This is equivalent to a barrier for the reverse process, which in this case corresponds to oxidative addition of H_2 to the metal center. Under these circumstances, a facile reverse reaction would not be expected. However, in several systems there is evidence that oxidative addition of D_2 can occur with little or no barrier. The earliest report of such processes was the observation in ion cyclotron resonance studies of the sequential reaction of CpRh-(η^3-C_3H_5)$^+$, formed initially by the dehydrogenation of CpRh-(2-propyl)$^+$ ion, with D_2 to incorporate four deuterium atoms into the π-allyl group.[6] More recently, ion cyclotron resonance studies indicate that $M(C_5H_6)^+$ (M = Fe, Co), generated either by dehydrogenation of cyclopentene or by double dehydrogenation of cyclopentane, undergoes six H/D exchanges in the presence of excess D_2.[7] Likewise, $Co(C_5H_6)^+$, produced by reaction of Co^+ with either cycloheptatriene or norbornadiene, is observed to exchange all six hydrogens for deuterium.[8] The first exchange occurs at about 5% of the Langevin collision rate,[9] and the remaining exchanges proceed with rates about 1 order of magnitude slower.[7]

A proposed mechanism for these exchange processes is depicted in Scheme I.[7,8] It involves exchange oxidative addition of D_2 to the metal center as a first step, followed by D transfer, initially to the endo position of the ring. This accounts for the first, rapid exchange. A rate-limiting 1,5-sigmatropic shift (exofacial migration) allows substitution at the remaining ring positions.[7,8]

In the present work, we examine the proposition that if no barrier exists for oxidative addition of hydrogen, then the reverse process, dehydrogenation, might exhibit a statistical KERD. This in turn would implicate a potential energy surface for the reductive elimination of hydrogen, which is very different from that suggested by earlier studies where nonstatistical kinetic energy release distributions were observed.

Emphasis is placed on dehydrogenations, believed to be reversible, that form $Fe(C_5H_6)^+$. If dehydrogenation is statistical, modeling the process with statistical theory yields an additional benefit. Since the model calculations are sensitive to only one unknown parameter, the reaction exothermicity, variation of that parameter to achieve a good fit to the experimental results can be used to estimate the heat of reaction. In this way, thermochemical information such as metal–ligand bond strengths, which are very difficult to determine by any other method, can be obtained. These methods are applied to Fe^+ bonding to cyclopentadiene and 1,3-cyclohexene.

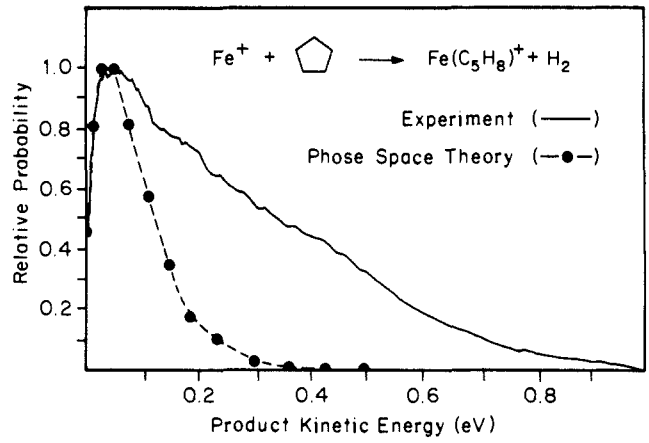

Figure 1. Experimental and theoretical kinetic energy release distribution, in the center-of-mass frame, for single dehydrogenation of cyclopentane by Fe^+.

Table I. Average Kinetic Energy Releases $\langle E_t \rangle$ from Experiment and Phase-Space Theory Calculations

reaction	$\langle E_t \rangle$[a] expt	theory
Fe^+ + ⬠ → $Fe(C_5H_8)^+$ + H_2	0.27	0.087[b]
Fe^+ + ⬠ → $[Fe(C_5H_8)^+]^*$ + H_2		
↳ $Fe(C_5H_6)^+$ + H_2	0.15[c]	*d*
Fe^+ + ⬟ → $Fe(C_5H_6)^+$ + H_2	0.14	0.14
Fe^+ + ⬡ → $Fe(C_6H_{10})^+$ + H_2	0.26	*e*
Fe^+ + ⬡ → $[Fe(C_6H_{10})^+]^*$ + H_2		
↳ $Fe(C_6H_8)^+$ + H_2	0.19[c]	*d*
Fe^+ + ⬡ → $Fe(C_6H_8)^+$ + H_2	0.15	0.15
Fe^+ + ⬡ → $[Fe(C_6H_8)^+]^*$ + H_2		
↳ $Fe(C_6H_6)^+$ + H_2	0.29[c]	*d*

[a] Units: eV. [b] Phase-space theory assuming ground-state Fe^+. The calculated average kinetic energy release for excited state $Fe^+(^4D)$ is 0.14 eV. [c] The average kinetic energy release is associated with the second H_2 elimination process. Initial H_2 elimination occurs in the ion source. [d] Not calculated because of the ambiguity in reactant internal energy. [e] Theoretical calculations were not done, but the estimated statistical average KER is on the order of 0.09 eV.

Experimental Section

Kinetic energy release measurements were carried out at UCSB with use of a double-focusing, reversed-geometry mass spectrometer (VG Industries, ZAB-2F),[10] with a home-built pressure- and temperature-variable electron impact source. The methods used in metastable dissociation studies have been described.[11] Briefly, Fe^+, from 150-eV electron impact on $Fe(CO)_5$, was allowed to react in the source with the hydrocarbon of interest to form a M(hydrocarbon)$^+$ adduct. Total source pressures were typically (1–5) × 10^{-3} Torr, monitored with a Baratron capacitance manometer. The ratio of $Fe(CO)_5$ and hydrocarbon pressures was approximately 1:1 and was varied to maximize adduct signal. The source temperature was maintained between −10 and 0 °C to minimize the decomposition of metal-containing compounds on insulating surfaces. Ions exiting the source were accelerated to 8 keV and mass selected with a magnetic sector. Fragment ions from metastable decomposition in the second field-free region (downstream from the magnet) were energy analyzed with an electrostatic sector and were detected

(5) van Koppen, P. A. M.; Jacobson, D. B.; Illies, A.; Bowers, M. T.; Hanratty, M. A.; Beauchamp, J. L. *J. Am. Chem. Soc.* **1989**, *111*, 1991–2001.
(6) Beauchamp, J. L.; Stevens, A. E.; Cordeman, R. R. *Pure Appl. Chem.* **1979**, *51*, 967.
(7) Jacobson, D. B.; Freiser, B. S. *J. Am. Chem. Soc.* **1983**, *105*, 7492–7500.
(8) Jacobson, D. B.; Byrd, G. D.; Freiser, B. S. *Inorg. Chem.* **1984**, *23*, 553–557.
(9) (a) Gioumousis, G.; Stevenson, D. P. *J. Chem. Phys.* **1958**, *29*, 294. (b) Su, T.; Bowers, M. T. In *Gas Phase Ion Chemistry*; Bowers, M. T., Ed.; Academic Press: New York, 1979; Vol. 1, Chapter 3.
(10) Morgan, R. P.; Beynon, J. H.; Bateman, R. H.; Green, B. N. *Int. J. Mass Spectrom. Ion Phys.* **1978**, *28*, 171–191.
(11) Jarrold, M. F.; Illies, A. J.; Bowers, M. T. *Chem. Phys.* **1982**, *65*, 19.

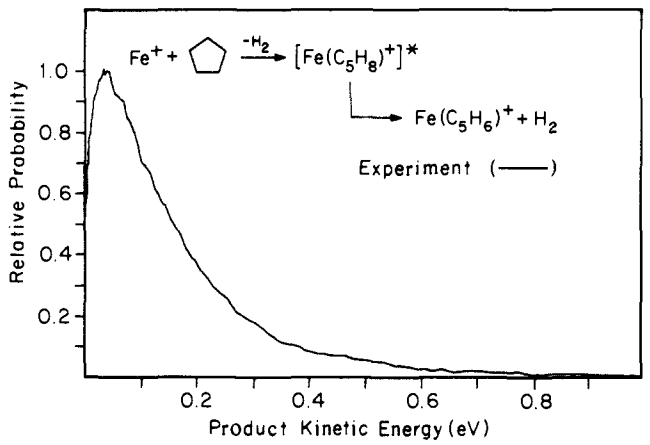

Figure 2. Experimental kinetic energy release distribution, in the center-of-mass frame, for double dehydrogenation of cyclopentane by Fe^+. Loss of the first H_2 molecule occurs in the ion source, and the measured distribution is for loss of the second H_2.

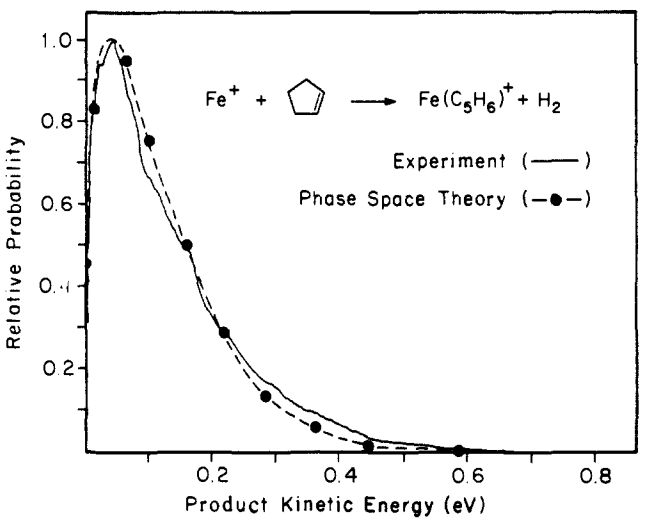

Figure 3. Experimental and theoretical kinetic energy release distribution, in the center-of-mass frame, for dehydrogenation of cyclopentene by Fe^+. The calculated distribution yields $D_0°(Fe^+–C_5H_6)$ = 50 kcal/mol.

by pulse-counting techniques. The background pressure in the second field-free region was typically less than 10^{-9} Torr, eliminating contributions from collision-induced dissociation to the metastable peaks. The resolution of the main ion beam was typically 0.5 eV fwhm. At this resolution, the contribution of the main-beam energy spread to the width of the kinetic energy release distribution in the center-of-mass reference frame is not important.[11] The methods for obtaining kinetic energy release distributions from metastable peak shapes have been described.[12] Raw data were smoothed by use of a moving average algorithm, after which numerical differentiation and conversion to the center-of-mass reference frame were carried out.

Results and Discussion

KERDs for dehydrogenations of cyclopentane, cyclopentene, cyclohexane, and cyclohexene are depicted in Figures 1–6. Experimental average kinetic energy releases for each process are compiled in Table I. Where appropriate, averages calculated with phase-space theory are also included in Table I.

$Fe(C_5H_8)^+$. Single dehydrogenation of cyclopentane, reaction 1, produces $Fe(C_5H_8)^+$. The KERD for this dehydrogenation process (Figure 1) is quite broad. Phase-space theory (see Appendix) was unable to produce a fit to the distribution (see Figure

$$Fe^+ + c\text{-}C_5H_{10} \rightleftarrows [Fe(C_5H_{10})^+]^* \rightarrow Fe(C_5H_8)^+ + H_2 \quad (1)$$

1). The inability to fit the experimental distribution with statistical theory, with a reasonable range of parameters, strongly suggests that this dehydrogenation process is nonstatistical, similar to those noted previously,[4,5] and suggests the presence of a barrier in the exit channel.

(12) (a) Jarrold, M. F.; Illies, A. J.; Bowers, M. T. *J. Chem. Phys.* **1983**, *79*, 6086. (b) Jarrold, M. F.; Illies, A. J.; Kirchner, J. J.; Wagner-Redeker, W.; Bowers, M. T.; Mandich, M. L.; Beauchamp, J. L. *J. Phys. Chem.* **1983**, *87*, 2213–2221.

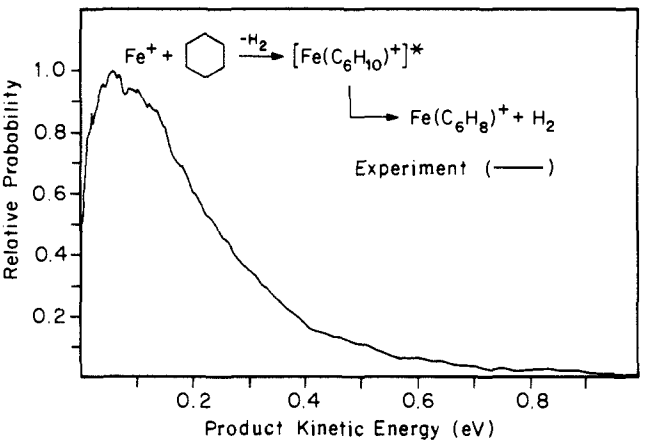

Figure 4. Experimental kinetic energy release distribution, in the center-of-mass frame, for double dehydrogenation of cyclohexane by Fe^+. Loss of the first H_2 molecule occurs in the ion source, and the measured distribution is for loss of the second H_2.

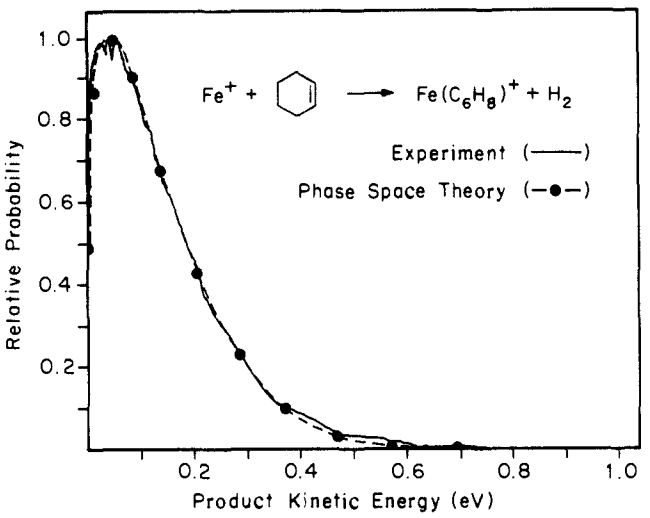

Figure 5. Experimental and theoretical kinetic energy release distribution, in the center-of-mass frame, for single dehydrogenation of cyclohexene by Fe^+. The calculated distribution yields $D_0°(Fe^+–C_6H_8)$ = 66 kcal/mol.

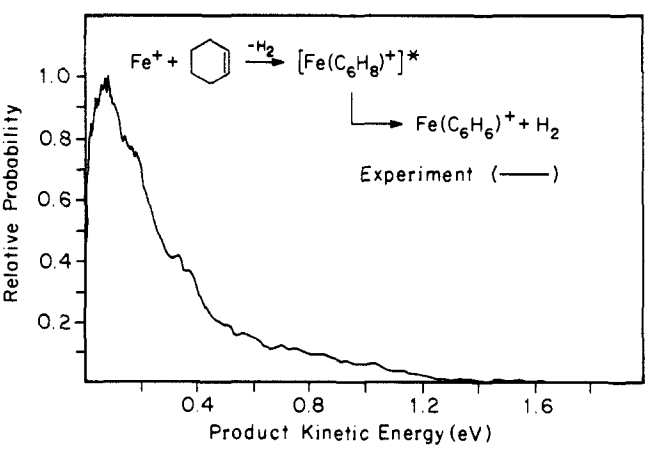

Figure 6. Experimental kinetic energy release distribution, in the center-of-mass frame, for double dehydrogenation of cyclohexene by Fe^+. Loss of the first H_2 molecule occurs in the ion source, and the measured distribution is for loss of the second H_2. Note the change in scale.

Scheme II. Proposed Mechanism for Dehydrogenation of Cyclopentene by a Transition-Metal Ion (M^+)

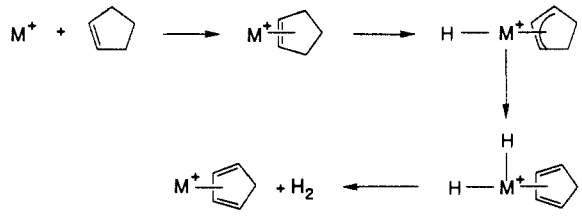

$Fe(C_5H_6)^+$. $Fe(C_5H_6)^+$ is formed by two successive dehydrogenations of cyclopentane, reaction 2, or by single dehydrogenation of cyclopentene, reaction 3. For reaction 2, the first H_2 loss occurs

$$Fe^+ + c\text{-}C_5H_{10} \rightarrow [Fe(C_5H_8)^+]^* + H_2 \rightarrow Fe(C_5H_6)^+ + H_2 \quad (2)$$

$$Fe^+ + c\text{-}C_5H_8 \rightleftharpoons [Fe(C_5H_8)^+]^* \rightarrow Fe(C_5H_6)^+ + H_2 \quad (3)$$

in the ion source and the mass-selected ion is $[Fe(C_5H_8)^+]^*$, which loses a second H_2 molecule via metastable reaction in the second field-free region of the mass spectrometer. The KERD measured for the loss of this second H_2 is shown in Figure 2. This process cannot be modeled with phase-space theory in a straightforward manner, since an important input parameter, the level of internal excitation of $[Fe(C_5H_8)^+]^*$, is unknown.[13] In reaction 3, the mass-selected ion is the Fe^+–cyclopentene adduct, and the phase-space treatment is straightforward since in this case the energetics are fully determined by the heats of formation of the reactants. The best fit, shown in Figure 3, yields a value of $D_0°(Fe^+$–cyclopentadiene$) = 50 \pm 5$ kcal/mol, where the estimated uncertainty reflects the sensitivity of the fit.[4] This result is in very good agreement with an upper limit value of 55 ± 5 kcal/mol derived from threshold photodissociation experiments.[15]

A mechanism for reaction 3 is suggested in Scheme II. Initially, a Fe^+–cyclopentene adduct is formed by coordination of the metal to the double bond. Transfer of a β-H results in a hydridoallylic species, which rearranges by a second H transfer to produce $H_2Fe^+(C_5H_6)$, which reductively eliminates hydrogen.

The similarity in both the overall shapes of the KERDs (Figures 2 and 3) and in the average kinetic energy releases for reactions 2 and 3 is striking. This result implies that the dissociating $[Fe^+–C_5H_8]^*$ ions are formed with similar internal energies from both sources, in addition to decomposing on the same potential surface. A schematic potential energy diagram showing the energetics of the various reactions is given in Figure 7. The first dehydrogenation step of reaction 2 is known to be exothermic since it proceeds rapidly in the gas phase.[16,17] Based on available data for M^+–alkene bonds,[18] this step is probably at least 10–15 kcal/mol exothermic for ground-state Fe^+ ions. Therefore, the first loss of H_2 in reaction 2 could leave the $Fe(C_5H_8)^+$ product with substantial internal excitation due to the exothermicity of the first step less the energy lost to H_2 rotation and vibration and to relative translation. The question is whether this is sufficient energy to promote the second H_2 loss with the KERD given in Figure 2.

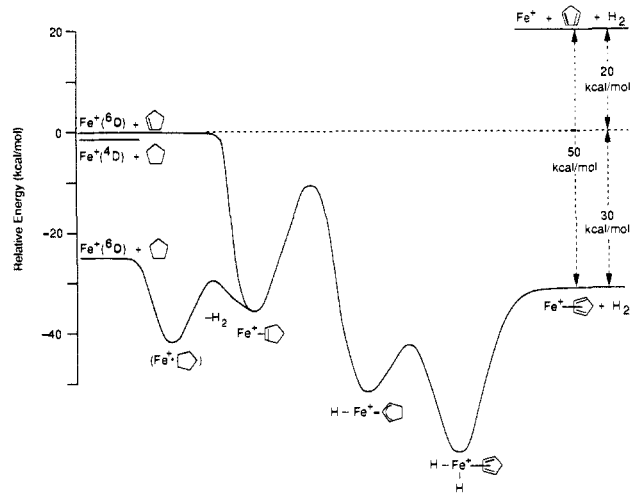

Figure 7. Schematic potential energy surface for the dehydrogenation reactions of Fe^+ with cyclopentane and cyclopentene, showing semiquantitative energetics for the various processes. Dehydrogenation of cyclopentane by electronically excited $Fe^+(^4D)$ yields a Fe^+–cyclopentene species with approximately the same internal energy as that formed when ground-state $Fe^+(^6D)$ associates directly with cyclopentene.

Reaction 3 is chemically activated by the energy of association of Fe^+ with cyclopentene, so the level of internal excitation of the $[Fe(C_5H_8)^+]^*$ produced should reflect the strength of the Fe^+–C_5H_8 bond, with none of the loss processes of reaction 2. Consequently, reaction 3 should produce $[Fe(C_5H_8)^+]^*$ metastables that, on average, are at least 23–25 kcal/mol more excited than those of reaction 2. How can the similarity in the KERDs for reactions 2 and 3 be reconciled with the expected differences in metastable energies for the two processes? If an adduct has a dissociation rate in the range 10^5–10^6 s^{-1}, it will give a very intense (relative to the main beam) metastable peak since this matches the temporal requirements for decomposition in the second field free region of the reverse geometry instrument. Ions with higher rates of dissociation decompose mainly in the source, and slower rates of dissociation allow the majority of adducts to reach the detector before decomposing. RRKM calculations[19,20] show that $[Fe(C_5H_8)^+]^*$ with an internal excitation of 35 kcal/mol above the dehydrogenation threshold (reaction 3) dissociates with a rate constant of about 10^6 s^{-1}, close to the most efficient rate for the time window of our experiment. On the other hand, $[Fe(C_5H_8)^+]^*$ produced from ground-state $Fe^+(^6D)$ via reaction 2 has a *maximum* of 17 kcal/mol above the threshold for the second dehydrogenation reaction. The calculated dissociation rate constant at this level of excitation is $\sim 2 \times 10^3$ s^{-1}, substantially smaller than optimum. Further, most of the $[Fe(C_5H_8)^+]^*$ generated in reaction 2 will have internal energies less than this and consequently will dissociate even more slowly. The metastable peak for reaction 2 should thus yield a KERD peaked at lower energies with lower average energy than the one expected from the much more highly excited $[Fe(C_5H_8)^+]^*$ generated in reaction 3.

One possible source of additional excitation in reaction 2 is electronically excited Fe^+. $Fe^+(^4D)$, derived from a $4s3d^6$ electronic configuration and lying 0.98 eV (differences in state energies are statistically weighted over J levels) above the $Fe^+(^6D)$ ground state (which is also derived from $4s3d^6$),[21] may be responsible for the KERD for reaction 2. As is noted in Figure 7, the level of excitation, 22.6 kcal/mol, is in approximately the right range to produce $[Fe(C_5H_8)^+]^*$ with internal energies similar to those

(13) In situations where the kinetics of the decomposition process as a function of internal energy are known (or can be adequately estimated), it is still possible to carry out the phase-space calculation of kinetic energy release by using the known lifetime of the metastable and the kinetics of its decomposition to back-calculate the internal energy of the metastable (see ref 14). However, the dehydrogenation processes of the current work were deemed too complex to be easily treated by this approach.

(14) Dearden, D. V.; Hayashibara, K.; Beauchamp, J. L.; Kirchner, N. J.; van Koppen, P. A. M.; Bowers, M. T. *J. Am. Chem. Soc.* **1989**, *111*, 2401–2409.

(15) Huang, Y.; Freiser, B. S. Personal communication.

(16) Byrd, G. D.; Burnier, R. C.; Freiser, B. S. *J. Am. Chem. Soc.* **1982**, *104*, 3565.

(17) Armentrout, P. B.; Beauchamp, J. L. *J. Am. Chem. Soc.* **1981**, *103*, 6628.

(18) $D_{298}°(Fe^+$–propene$)$ has been estimated at 37 ± 2 kcal/mol,[7] and $D_0°(Co^+$–propene$)$ has been determined to be 44 ± 5 kcal/mol.[4]

(19) Marcus, R. A.; Rice, O. K. *J. Phys. Colloid Chem.* **1981**, *55*, 894. Marcus, R. A. *J. Chem. Phys.* **1952**, *20*, 359. Robinson, J. P.; Holbrook, K. A. *Unimolecular Reactions*; Wiley: New York, 1972. Forst, W. *Theory of Unimolecular Reactions*; Academic: New York, 1973.

(20) Calculations were performed by use of "A General RRKM Program", by W. L. Hase and D. L. Bunker, with the following parameters: log A = 12.71, reaction threshold = 40 kcal/mol, state counting with the Whitten–Rabinovitch approximation.

(21) Corliss, C.; Sugar, J. *J. Phys. Chem. Ref. Data* **1982**, *11*, 135–241.

Scheme III. Proposed Mechanism for H/D Exchange in $M(C_5H_6)^+$ Species, Where Reversible Interconversion of M^+–Diene and M^+–π-Allylic Structures Accounts for the Initial Exchange

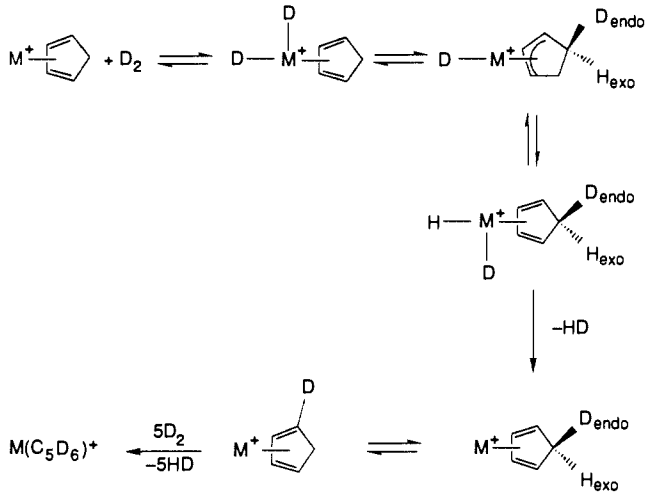

expected in reaction 3. Mobility studies indicate that as much as 50% of the Fe^+ ions produced by electron impact on $Fe(CO)_5$ is electronically excited,[22] of which the excited $3d^7$ configurations are deactivated relatively quickly by collisions with helium.[23] The excited $Fe^+(^4D)$ state, however, has a $4s3d^6$ configuration that will not deactivate under our experimental conditions.[22] In addition, several experiments imply that a significant fraction of the electronically excited Fe^+ is reactive. For example, the reaction of Fe^+ with methanol to generate $FeOH^+$ and methyl radical is believed to be 0.70 ± 0.20 eV endothermic for ground-state species but has been observed for Fe^+ produced by electron impact on $Fe(CO)_5$.[24] The observation was explained by postulating that approximately 3% of the Fe^+ was formed in a long-lived excited state at least 0.5 eV above the ground state, which upon interaction with methanol can quickly cross to the ground-state potential energy surface.[25] Highly excited states of Fe^+ have also been observed by Loh et al.[26] in reactions with O_2 and c-C_2H_4O when Fe^+ is made by high-energy electron impact on $Fe(CO)_5$ or by laser vaporization of metallic iron. It is therefore reasonable to conclude that the excited-state $Fe^+(^4D)$ rather than the ground-state $Fe^+(^6D)$ is responsible for the double dehydrogenation of cyclopentane. Other excited states may also be present. If our analysis is correct, states at higher and lower energies will lead to adduct dissociation rates that do not contribute significantly to the observed metastable.

Electronically excited Fe^+ can also be involved in reaction 3. In this instance, however, the degree of excitation is great enough that most of the $[Fe^+ \cdot C_5H_8]^*$ species will dissociate before reaching the second field-free region of the instrument and thus will not significantly contribute to the metastable peak from which the KERD is derived. Furthermore, if electronically excited Fe^+ made a significant contribution to the KERD for reaction 3, it would be unlikely that the phase-space analysis would give an excellent fit with a *single* value of the assumed internal excitation.

The *statistical* kinetic energy release distribution observed for H_2 elimination from $Fe(C_5H_8)^+$ indicates that oxidative addition of H_2 to the metal center occurs without an activation energy barrier. This result is supported by the fact that $Fe(C_5H_6)^+$ undergoes six H/D exchanges in the presence of excess D_2. The mechanism for the H/D exchange process is still in question. Earlier work[7,8] postulated that $Fe(C_5H_6)^+$ reversibly rearranges from $Fe^+(C_5H_6)$ to the hydridocyclopentadienyl species, on the basis of the observation of H/D exchange. The ability to assess the importance of such processes is difficult since not enough thermochemical data are available to estimate the relative stabilities of the two species. An alternative to the mechanism proposed in Scheme I for the H/D exchange process is suggested in Scheme III, involving a reversible hydrogen shift from the metal to the diene to give a π-allylic structure. This mechanism invokes oxidative addition of hydrogen to give the same structure as in the dehydrogenation mechanism. The KERD results (Figure 3) are consistent with the absence of a barrier to this process. The remaining steps are the same as in Scheme I. Scheme III is consistent with the observed H/D exchange kinetics, the initial exchange being rapid and the rate of the remaining exchange being limited by the rate of the sigmatropic shift. Further, Scheme III explains the results without resorting to the high metal oxidation state of the H_3Fe^+–cyclopentadienyl structure implicit in Scheme I.

$Fe(C_6H_{10})^+$. Single dehydrogenation of cyclohexane, reaction 4, produces $Fe(C_6H_{10})^+$. The KERD for this dehydrogenation

$$Fe^+ + c\text{-}C_6H_{12} \rightleftharpoons [Fe(C_6H_{12}^+)]^* \rightarrow Fe(C_6H_{10})^+ + H_2 \quad (4)$$

process is quite broad and resembles the nonstatistical KERD for single dehydrogenation of cyclopentane, shown in Figure 1. Again, the nonstatistical distribution suggests the presence of a barrier in the exit channel.

$Fe(C_6H_8)^+$ and $Fe(C_6H_6)^+$. $Fe(C_6H_8)^+$ is generated in double dehydrogenation of cyclohexane, reaction 5, or single H_2 loss from cyclohexene, reaction 6. The same considerations apply to re-

$$Fe^+ + C_6H_{12} \rightarrow [Fe(C_6H_{10})^+]^* + H_2$$
$$\hookrightarrow Fe(C_5H_8)^+ + H_2 \quad (5)$$

$$Fe^+ + C_6H_{10} \rightleftharpoons [Fe(C_6H_{10})^+]^* \rightarrow Fe(C_6H_8)^+ + H_2 \quad (6)$$

action 5 as to reaction 2. The KERD for the loss of the second H_2 molecule in reaction 5 is shown in Figure 4. This process was not modeled since the $[Fe(C_6H_{10})^+]^*$ internal energy is not well-defined. A mechanism analogous to that presented in Scheme II, based on successive β-H transfers followed by reductive elimination, is assumed to account for reaction 6, which yields the KERD shown in Figure 5. The KERD for H_2 loss to form $Fe(C_6H_6)^+$ (reaction 7, Figure 6) is relatively broad, indicating a

$$Fe^+ + C_6H_{10} \rightarrow [Fe(C_6H_8)^+]^* + H_2$$
$$\hookrightarrow Fe(C_6H_6)^+ + H_2 \quad (7)$$

substantial exit-channel barrier, an unusually large exothermicity, or both. The binding energy of Fe^+ to benzene has been estimated in several studies[27] to be in the range 55–58 kcal/mol. The double dehydrogenation of cyclohexene to yield benzene is endothermic by 21 kcal/mol, making the overall reaction exothermic by 36 kcal/mol or 1.6 eV for ground-state Fe^+. The maximum kinetic energy release of ~1.3 eV in Figure 6 approaches this value.

Formation of $Fe(C_6H_8)^+$ via reactions 5 and 6 produces KERDs that are distinct, with that from reaction 5 being slightly broader. If the metastable decomposition occurs on the same surface for both reactions, this result suggests excited-state Fe^+ participation is important in reaction 5 to account for excess energy in the $[Fe(C_6H_{10})^+]^*$ metastable, analogous to reaction 2.

The results of phase-space modeling of reaction 6 are included in Figure 5. The good fit between theory and experiment supports the contention that this is a further example of statistical energy partitioning to product degrees of freedom in a dehydrogenation process. The value of $D_0°(Fe^+–C_6H_8)$ derived from the fit is 66 $\pm$ 5 kcal/mol. It is interesting to note that this bond energy is greater than the bond energy for benzene to iron, $D_0°(Fe^+–C_6H_6)$,

(22) Kemper, P. R.; Bowers, M. T. To be published.
(23) The deactivation rate for the excited $3d^7$ configuration states were measured to be 6×10^{-14} cm^3/molecule-s (ref 22).
(24) (a) Allison, J.; Ridge, D. P. *J. Am. Chem. Soc.* **1976**, *98*, 7445–7446. (b) Allison, J.; Ridge, D. P. *J. Am. Chem. Soc.* **1979**, *101*, 4998–5009.
(25) Reents, W. D., Jr.; Strobel, F.; Freas, R. B., III; Wronka, J.; Ridge, D. P. *J. Am. Chem. Soc.* **1985**, *89*, 3666–3670.
(26) Loh, S. K.; Fisher, E. R.; Lian, L.; Schultz, R. H.; Armentrout, P. B. *J. Chem. Phys.* **1989**, *93*, 3159.
(27) (a) Hettich, R. L.; Jackson, T. C.; Stanko, E. M.; Freiser, B. S. *J. Am. Chem. Soc.* **1986**, *108*, 5086. (b) Jacobson, D. B.; Freiser, B. S. *J. Am. Chem. Soc.* **1984**, *106*, 3900.

Table II. Input Parameters Used in Calculations

	cyclopentane	cyclopentene	cyclohexene	Fe^+–cyclopentene	Fe^+–cyclopentadiene	Fe^+–cyclohexadiene
B^a	0.175	0.198	0.127	0.100	0.111	0.100
σ^b	10	2	2	1	1	1
α^c	9.235	9.010	10.853			
ν_i^d	2966 (2)	3060	3060	3060	3080	3060
	2960	3039	3039	3039	3012 (3)	3039
	2949 (2)	2967	2967	2967	2982	2967
	2906	2958	2916	2958	2900	2916
	2904 (2)	2927	2958	2927	1644	2958
	2890 (2)	2916	2927	2916	1640	2927
	1456 (2)	2898	2900 (2)	2898	1413	2898
	1453 (3)	2849	2898	2849	1314	2849
	1350 (2)	1614	2849	1614	1295	1614
	1316 (2)	1468 (2)	1614	1468 (2)	1120	1468 (2)
	1311	1441	1468 (2)	1441	1060	1460
	1295	1432	1460	1432	995 (3)	1441
	1283 (2)	1356	1441	1356	920	1432
	1207 (2)	1302	1432	1302	918	1356
	1030 (2)	1297 (2)	1356	1297 (2)	876	1302
	1004 (2)	1284	1302	1284	760	1297 (2)
	896 (2)	1207 (2)	1297 (2)	1207 (2)	721	1284
	886	1108	1284	1108	700	1207 (2)
	717 (2)	1082	1207 (2)	1082	600	1108
	628 (2)	1027	1200 (2)	1027	562	1082
	546 (2)	965	1108	965	500	1027
	283	937	1082	937	421 (2)	965
		900	1027	900	331	937
		800	965	800	137	900 (3)
		772	950 (2)	772	102	800
		702	937	702		772
		692	900 (3)	692		702
		603	800	603		700
		387	772	600		692
		254	702	500		603
			692	400		600
			603	387		500
			387	254		387
			254			254

[a] Rotational constants in cm^{-1}. [b] Symmetry numbers. [c] Polarizabilities in $Å^3$. [d] Vibrational frequencies in cm^{-1}.

which was measured by Hettich et al. to be 55 ± 5 kcal/mol.[27a]

A final comment involves the relative strengths of $D_0°(Fe^+–C_5H_6)$ and $D_0°(Fe^+–C_6H_8)$. Assuming (as seems likely) that both ligands are conjugated dienes, it it interesting that C_6H_8 binds Fe^+ 16 kcal/mol more strongly than C_5H_6. Condensed-phase η^4-butadiene complexes of Fe are well-known, strongly bound species,[28] which can perhaps be used as models of the lowest energy geometry for a diene ligand bound to metal. The C–C–C angle of the butadiene ligand in (η^4-butadiene)tricarbonyliron has been determined to be 118° by use of X-ray diffraction,[29] somewhat compressed from the 122.4° found by use of electron diffraction for free butadiene in the gas phase.[30] Similarly compressed butadiene bond angles are found for several η^4-butadiene complexes of neutral Mn,[31] where the C–C–C angles in the diene unit are in the range 118.8–119.6°. The structure of solid-phase cyclopentadiene has been determined with X-ray techniques.[32] The ring is planar and quite distorted from ideal pentagonal geometry; the C–C–C bond angles of the diene unit are 112 and 107°. The corresponding bond angles in gaseous 1,3-cyclohexadiene are each 120.1°, measured with use of electron diffraction.[33] The similarity of the bond angles in free 1,3-cyclohexadiene and 1,3-butadiene bound to metal, combined with the higher bond energy found for C_6H_8, suggests that the geometry of 1,3-cyclohexadiene is better suited for formation of a strong bond to Fe^+ than is the distorted geometry of cyclopentadiene.

Table III. Heats of Formation Used in This Work

species	heat of formation, kcal/mol 0 K	298 K
Fe^+	280.4[a]	281[a]
cyclopentane	−10.6[a]	−18.7[a]
cyclopentene	14.5[a]	8.6[a]
cyclopentadiene	34.9[a]	31[a]
cyclohexane	−19.5[a]	−29.5[a]
cyclohexene	6.9[a]	−1.1[a]
1,3-cyclohexadiene	31.1[a]	25.4[a]
benzene	24.0[a]	19.8[a]
Fe^+–cyclopentadiene	265[b]	259[c]
Fe^+–cyclohexadiene	246[b]	240[c]

[a] Lias, S. G.; Bartmess, J. E.; Liebman, J. F.; Holmes, J. L.; Levin, R. D.; Mallard, W. G. *J. Phys. Chem. Ref. Data* **1988**, *17*, Supplement No. 1. Corrections of values listed at 298 to 0 K values were made where necessary. [b] Derived from single-parameter fit of kinetic energy release distribution predicted with phase-space theory to experimental distribution, as discussed in text. The estimated uncertainty is ±5 kcal/mol, reflecting the sensitivity of the fit. [c] Heat of formation at 298 K estimated from the 0 K value.

Conclusion

The results given in this paper make it clear that a particular metal ion, in this case Fe^+, can exhibit a full range of behavior for oxidative addition of hydrogen, depending mainly on the ligand environment. When bound to cyclopentadiene or cyclohexadiene, oxidative addition of hydrogen to the metal center is facile. This is not the case when Fe^+ is ligated by a single olefin, however. Kinetic energy release distributions provide the means for readily distinguishing contrasting potential energy surfaces for organometallic reactions, and in this case for extracting Fe^+–diene bond

(28) Collman, J. P.; Hegedus, L. S.; Norton, J. R.; Finke, R. G. *Principles and Applications of Organotransition Metal Chemistry*; University Science Books: Mill Valley, CA, 1987.
(29) Mills, O. S.; Robinson, G. *Acta Crystallogr.* **1963**, *16*, 758–761.
(30) Almenningen, A.; Bastiansen, O.; Traeteberg, M. *Acta Chem. Scand.* **1958**, *12*, 1221–1225.
(31) Harlow, R. L.; Krusic, P. J.; McKinney, R. J.; Wreford, S. S. *Organometallics* **1982**, *1*, 1506–1513.
(32) Liebling, G.; Marsh, R. E. *Acta Crystallogr.* **1965**, *19*, 202–205.
(33) Oberhammer, H.; Bauer, S. H. *J. Am. Chem. Soc.* **1969**, *91*, 10–16.

dissociation energies when modeled by statistical phase-space theory.

Acknowledgment. We thank the National Science Foundation for supporting this research through Grants CHE87-11567 (J.L.B.) and CHE88-17201 (M.T.B.). We are also grateful to the Shell Foundation for graduate fellowship funding (D.V.D.) and to the donors of the Petroleum Research Fund, administered by the American Chemical Society, for additional support. We also thank Denley Jacobson for taking some of the original data.

Appendix

Calculation of kinetic energy release distributions, with use of phase-space theory to model the decomposition of metastable ions, requires a number of input parameters. The calculations are fairly insensitive to the parameters listed in Table II, including rotational constants B, symmetry parameters σ, neutral polarizabilities α, and vibrational frequencies ν_i. Values of B were taken from the literature where available[34] or calculated from typical Fe$^+$–C, C–C, and C–H bond lengths. Polarizabilities were estimated with the atomic hybrid components method.[35] Vibrational frequencies were taken from literature[36] where possible or estimated from literature values of similar species. The estimated frequencies were varied over the entire physically reasonable range for these quantities and were found not to affect the details of the kinetic energy release distributions over this range.

The phase-space calculations are quite sensitive to the total energy available for partitioning among the various modes and, hence, to the heats of formation of the reactants and products. The values employed are listed in Table III. As noted in the Results and Discussion, in cases where the heats of formation of all reactants and products save one are known, the remaining heat of formation can be determined by varying it as a free parameter to achieve a fit of the calculated results to the experimental measurements. This method was used to obtain the values for the organometallic ions reported in Table III.

(34) Landolt-Bornstein, H. H. *Numerical Data and Functional Relationships in Science and Technology, New Series, Group II*; Hellwege, K. H., Hellwege, A. M., Eds.; Springer-Verlag: Berlin, 1974, 1976; Vols. 6, 7.

(35) Miller, K. J.; Savchik, J. A. *J. Am. Chem. Soc.* **1979**, *101*, 7206–7213.

(36) (a) Shimanouchi, T. *Table of Molecular Vibrational Frequencies*; National Bureau of Standards: Washington, DC, 1972; Consolidated Vol. 1. (b) Sverdlov, L. M.; Kovner, M. A.; Krainov, E. P. *Vibrational Spectra of Polyatomic Molecules*; Wiley: New York, 1970.

Comparative Study of Resonance Raman and Surface-Enhanced Resonance Raman Chlorophyll *a* Spectra Using Soret and Red Excitation

Lana L. Thomas, Jae-Ho Kim, and Therese M. Cotton*

Contribution from the Department of Chemistry and Ames Laboratory, Iowa State University, Ames, Iowa 50011. *Received April 9, 1990. Revised Manuscript Received August 3, 1990*

Abstract: Surface-enhanced resonance Raman scattering (SERRS) spectra are reported for chlorophyll *a* adsorbed on a silver electrode at 298 and 77 K with 406.7-, 457.9-, 514.5-, and 647.1-nm excitation. Submerging the electrode in degassed water at 298 K was found to improve the spectral quality by minimizing sample heating and photooxidation. Spectral intensities and peak resolutions were greater at all excitation wavelengths at liquid nitrogen temperature. Most significantly, roughened silver at the low temperature quenched the fluorescence accompanying red excitation and minimized sample photooxidation, resulting in richly detailed SERRS spectra of chlorophyll *a*. The close correspondence between chlorophyll *a* resonance Raman (RR) and SERRS spectra suggests that an electromagnetic mechanism is the major source of the surface enhancement, rather than a chemical mechanism (e.g. a charge-transfer complex between chlorophyll *a* and the metal). The spectral similarities, together with the presence of the MgN_4 vibration band in the SERRS spectra, also provide evidence that structural alterations (e.g. cleavage of ring V or loss of Mg) do not occur in chlorophyll *a* after adsorption at the electrode surface. A distinctive SERRS spectrum was obtained for each excitation wavelength. Selective excitation within the various electronic transitions can thus be utilized to verify assignments of the vibrational modes of chlorophyll *a* and to monitor its interactions and photochemical behavior in biomimetic systems.

Introduction

Chlorophyll *a* (Chl *a*) plays an essential role in the conversion of sunlight into chemical energy in green plants and blue green algae. Chlorophylls are metallochlorins (dihydrogen-reduced metalloporphyrins) found in photosynthetic membranes. The obligatory presence of metalochllorins in lieu of metalloporphyrins in photosynthetic and certain other biological systems is not understood. However, in an attempt to elucidate the structural and photochemical behavior of these compounds, resonance Raman (RR) spectroscopy has been utilized as a probe of the vibrational and electronic structure of metalloporphyrins[1-4] and, more recently, metallochlorins and chlorophylls.[5-12] The latter species result from reduction of the $C_b{=}C_b$ bond of ring IV of the porphyrin macrocycle. This destroys the in-plane degeneracy and has a profound effect on the electronic absorption spectrum. The typical B and Q electronic transitions of symmetrical porphyrins are split into x and y components. In addition, the Q transition gains considerable intensity relative to that observed in porphyrins.

The differences in the chlorin electronic properties are reflected in their RR spectra, which are strongly affected by excitation conditions. Resonance Raman excitation within the strongly allowed B transition results in enhancement of symmetric, in-plane modes arising primarily from Franck–Condon type scatter-

* Author to whom correspondence should be addressed.

(1) Johnson, B. B.; Peticolas, W. *Annu. Rev. Phys. Chem.* **1976**, *27*, 465–491.

(2) Spiro, T. G.; Stein, P. *Annu. Rev. Phys. Chem.* **1977**, *28*, 501–521.

(3) Felton, R. H.; Yu, N.-T. In *The Porphyrins*; Dolphin, D., Ed.; Academic Press: New York, 1978; Vol. II, pp 341–388.

(4) Spiro, T. G. In *Iron Porphyrins*; Lever, A. B. P., Gray, H. B., Eds.; Addison-Wesley: Reading, MA, 1982; Part II, pp 89–152.

0002-7863/90/1512-9378$02.50/0